Hydrogen induced stress cracking in heterogeneous materials

G. Chai[1, 2a]*, R. Lin Peng[2b], S. Johansson[2c] and U. Kivisäkk[1d]

[1]Sandvik Materials Technology, R&D Centre, S-811 81 Sandviken, Sweden

[2]Dept of Mechanical Engineering, Linköping University, S-581 83 Linköping, Sweden

[a]guocai.chai@sandvik.com, [b]Ru.Peng@liu.se, [c]sten.johansson@liu.se, ulf.kivisakk@sandvik.com

Keywords: Hydrogen induced cracking, Heterogeneous materials, Hydrogen embrittlement, EBSD, Creep, Duplex stainless steels.

Abstract. Duplex stainless steel (DSS) that has a heterogeneous microstructure of austenite and ferrite suffers from hydrogen induced stress cracking, HISC, in subsea applications. In this study, the HISC behaviors in three super duplex stainless steels with different microstructures have been investigated by a simulated HISC test, combined with SEM and EBSD analysis. HISC in duplex stainless steels is strongly dependent on the material composition, microstructure and loading conditions. HISC is a result of the interaction between the static and dynamic plasticity and hydrogen diffusion. It is observed that HISC damage (voids) can occur in both austenitic and ferritic phases and at both grain boundaries and phase boundary depending on plastic deformation introduced by both loading and then creep process and hydrogen diffusion during the HISC test. Deformation in duplex stainless steels is very heterogeneous in micro scale depending on material chemical compositions. Whether austenite or ferrite becomes the weaker phase during loading depends on not only the composition, but also the deformation hardening rate. The crack propagation paths in the DSS during HISC are discontinuous. The fracture surface consists of the cleavage ferritic phase and the valleys or peaks of the austenitic phase. This is mainly due to the heterogeneous mechanical behavior of these two phases.

Introduction

Steel material such as duplex stainless steels (DSS) used in subsea industry have been found to suffer from hydrogen induced stress cracking, HISC. This usually happened in a component with a cathodic protection [1, 2]. Different from the conventional hydrogen embrittlement, HE, HISC is a hydrogen diffusion related, localized cracking process. The occurrence of HISC needs a hydrogen source, a tensile stress and a material susceptible to hydrogen. Considerable amount of research work has been done to study the HISC behavior in different duplex steel grades and the influence of microstructure and deformation in the materials [2-7].

It is generally accepted that hydrogen-enhanced localized plasticity (HELP), hydrogen-enhanced decohesion (HEDE), and adsorption-induced dislocation emission (AIDE) are three principal mechanisms for HE or HISC in metals [8]. However, these three mechanisms usually occur with one of them being the dominant process depending on the fracture mode. In a heterogeneous material such as duplex stainless steel of austenite and ferrite which has an equal amount of austenitic phase and ferritic phase that have heterogeneous deformation behaviors [10, 11], the actual mechanisms of HISC are still not quite understood. Oltra R et al. [3] has studied the cracking mechanism in the austenitic phase and concluded that the transition of the crack propagation from the ferrite to the austenite induces localized microcracking of the austenitic grains following the mechanism of HELP. The movement of the dislocations is enhanced by hydrogen and the

dislocations will pile up ahead the diffusion zone and produce a virtual obstacle. The fracture process will result from a competition between the kinetics of dislocation emission and the kinetics of diffusion and at a critical level, a crack can start in the austenite. HISC due to the interaction between hydrogen and dislocations was proposed in a plastic deformed DSS. HISC can take place in the ferrite, but initiate as a result of the dislocation pile ups in the adjacent austenite phase [3]. Recently, Chai and his colleagues [7] proposed a local creep model for HISC in duplex stainless steels. HISC in DSS is a result of the interaction between the dynamic plasticity due to a creep process and hydrogen diffusion, which may occur for loading not only beyond but also below the yield stress of the DSS steel.

In this study, the HISC mechanisms in three DSS will be further discussed based on the earlier work [7] by using electron backscattered diffraction (EBSD) technique. The purpose is to have a better understanding on the mechanisms of HISC in heterogeneous materials. With EBSD technique [12], the stress/strain fields or dislocation density in the austenite and the ferrite of the hydrogen charged DSS, possible crack initiation location and cracking paths, can be analyzed. A model on the formation of microstresses in the austenitic phase and the ferritic phase under a constant load (in the creep condition) was proposed. This may help us to understand why HISC propagation occurs mainly in the ferritic phase.

Materials and experimental

Three commercial duplex stainless steels: SAF 2205, SAF 2507 and SAF 2906 were used in this study. As shown in Table 1, SAF 2906 containing higher amounts of N has a much higher hardness in the austenite. SAF 2507 containing a higher amount of Mo shows a higher hardness in the ferrite, but not much. SAF 2205, however, has a composition that shows the similar hardness in both phases. Loading in the Table 1 is the applied stress for the HISC test, which was given as a percentage of the bulk yield strength of the materials.

Table 1: Nominal chemical compositions and information of DSS used

Materials	C	Si	Mn	Cr	Ni	Mo	N	PRE	Hardness (Hv)		Loading
									austenite	ferrite	%Rp0,2
SAF 2205	0.03	1.0	2.0	22	5	3.2	0.18	35	246	243	130
SAF 2507	0.03	0.8	1.2	25	7	4.8	0.3	42	276	288	100
SAF 2906	0.03	0.3	0.47	29	6	2	0.4	42	351	299	120

The procedure for the simulated HISC test has been detailed elsewhere [6]. Here only a brief description is given. Cylindrical test specimens with a dimension of 3 mm diameter, a total length of 100 mm and a gauge length of 25.4 mm were taken from a longitudinal direction of the bar materials. All specimens, as a cathode in an electrochemical cell and a solution of 10% H_2SO_4, with 30 mg/l As_2O_3 added as the electrolyte, were then precharged with hydrogen using galvanostatic polarization at 20 mA/cm^2 for 24 hours. The HISC testing began immediately after the precharging using a constant load equipment with a dead weight. The temperature was set to 4 ± 1°C and was recorded. The electrolyte in the test cell was a 3% NaCl solution with a slow ingress of air. Cathodic protection was conducted potentiostatically at an applied potential of -1050 mV (SCE). A constant load related to the yield strength $R_{p0.2}$ was applied to the specimens.

After testing, the fracture mechanisms of HISC in DSS samples were investigated using SEM and EBSD. The EBSD analysis was carried in a Hitachi SU-70 scanning electron microscope with EBSD detector from Oxford Instrument and Channel 5 software. A length-wise cross section of specimen was carefully ground and polished to avoid residual plastic deformation due to sample preparation.

To evaluate the heterogeneous properties of the material, the microhardness of the individual phases was measured in the samples in as delivered condition as well as in samples with up to 30% cold deformation.

Results and discussion

Micro heterogeneous deformation behavior in duplex stainless steels. Fig. 1 shows influence of cold deformation on microhardness of the individual phases in these three DSS. They actually show the micro deformation behaviors of the individual phases. For SAF 2205 material, the increase of hardness in individual phases with cold deformation is similar, and therefore they show similar hardness up to 15% cold deformation. This indicates that these two phases have also similar deformation hardening rate since the original hardness of these two phases (without cold deformation) are similar as shown in Table 1. For SAF 2507 material, the behavior is quite different. Since the austenitic phase has a higher deformation hardening rate than the ferritic phase, the hardness of the austenitic phase after about 7% cold deformation is higher than that of the ferritic phase although the original hardness of the ferritic phase is slightly higher. For SAF 2906 containing 0.4% nitrogen, the hardness of the ferritic is always lower than that of the austenite even after 30% cold deformation. This is mainly due to the fact that nitrogen is always concentrated in the austenitic phase, which leads to a higher strength or hardness and also a higher deformation hardening rate. The results above show that the micro deformation behavior in a duplex stainless steel is very different and strongly dependent upon the chemical composition of the individual phase. Nitrogen content is a strong factor affecting the deformation behavior in the material. Similar results have been reported by a multiscale material modeling [10].

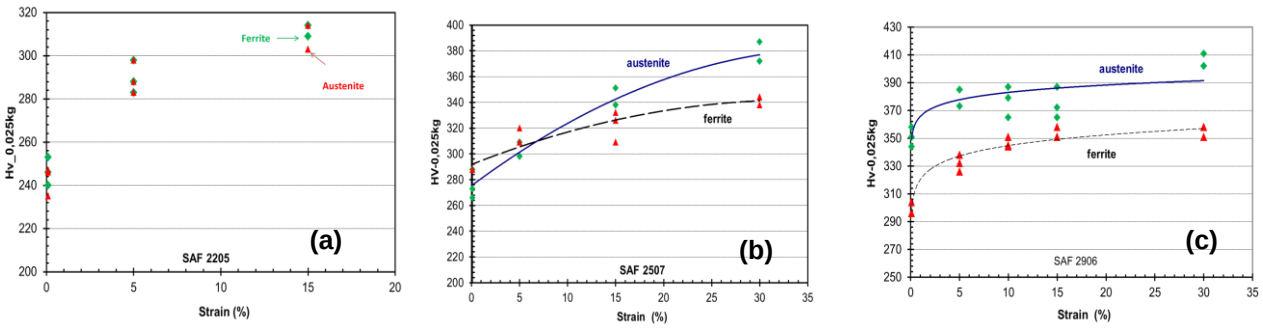

Fig. 1 Influence of cold deformation on microhardness of three duplex stainless steels, (a). SAF 2205, (b). SAF 2507, (c). SAF 2906.

Hydrogen induced stress cracking damage (voids). In the earlier paper [7], two types of crack initiations have been observed in DSS materials after the HISC test. One is the formation of small voids or pores at the ferritic grain boundaries, leading to microcracking in the ferritic phase. Another is that small pores have formed at the phase boundaries, which leads to the formation of small cracks inside the ferritic phase. Fig. 2 shows the damage or crack initiation (void) behavior of HISC in these three materials. It can be seen that damages or voids (the green area) can be observed in both austenitic and ferritic phase in SAF 2205 material (Fig. 2a). In SAF 2507 material, the damages are mainly in the ferritic phase, but few in the austenitic phase. Some crack initiation can also be observed, which has been reported earlier [7] (Fig. 2b). For SAF 2906 (Fig. 2c), the damages are mainly in the ferritic phase, but can also be observed in the austenitic phase. The cracks stopped in the austenitic phase. Fig. 2d-f show the EBSD mappings of the stress or strain conditions in the same samples. It can be seen that the damage areas are not always the highest stress or strain concentration areas. This can be attributed to the stress relaxation after the formation of damage or crack initiation, especially at grain or phase boundaries. For SAF 2205 (Fig. 2d), high stress or strain can be observed in the austenitic phase where the damages can be observed. In Fig. 2e (SAF 2507), the damage in the ferritic phase in some areas can be correlated to the stress or strain concentration. These results indicate that HISC process is a stress or strain accumulation process. When the stress or strain is high

enough, a damage or crack initiation can occur, which will consequently cause a stress or strain relaxation. For SAF 2507 material, high stress concentration in the ferritic phase can be related to its large grain size.

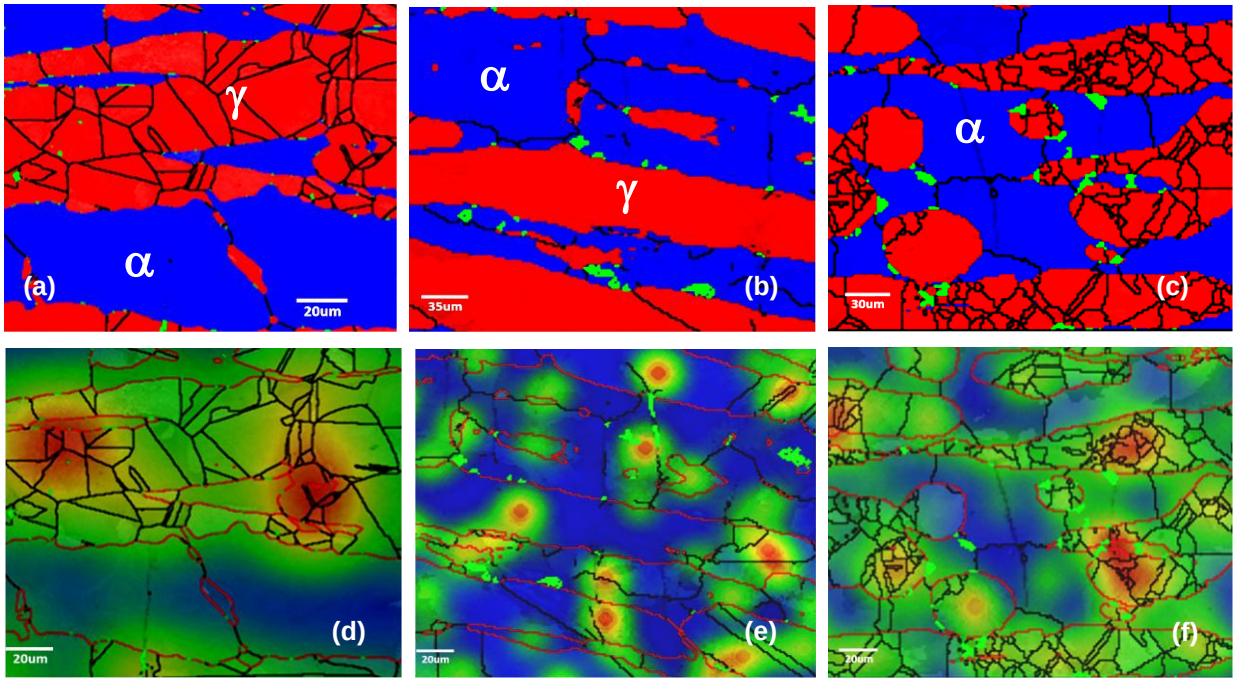

Fig. 2 EBSD mapping; (a)-(c). Formation of damage or voids (green ones). (d)-(f). Strain mapping with red color for high strain or stress and blue for low strain or stress; (a) and (d). SAF 2205, (b)-(e). SAF 2507, (c) and (f). SAF 2906.

Crack formation and path in duplex stainless steels. Fig. 3 shows some crack formation in the HISC tested samples. SAF 2205 material (Fig. 3a) shows very few microcracks that may initiate either in austenite or ferrite and propagate about one to two grain layers. In the regions near the facture surface, large plastic deformation appears. This may be attributed to the high applied stress, 130% of the bulk yield strength. The HISC is also observed to grow somewhat deeper in the austenite and in certain cases, it may go through the austenitic grain in a ductile manner, which can explained by hydrogen-enhanced localized plasticity (HELP) [3, 8].

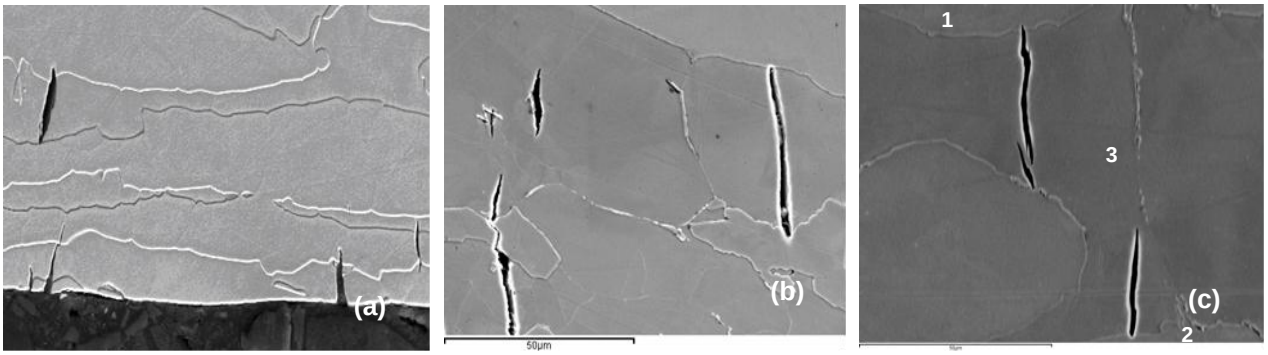

Fig. 3. HISC or crack path in duplex stainless steels, (a). SAF 2205, (b). SAF 2507, (c). SAF 2906.

For SAF 2507, denser and longer cracks are observed in some regions (Fig. 3b), in which cracking both at surface and in a depth up to 0.4 mm is observed. Surface cracks start often from ferrite grains but initiation at austenite is also found, while internal cracks initiate at phase boundary or inside

ferritic grains. Cracks propagate in ferrite grains and are often stopped or deflected by phase boundaries.

In comparison with SAF 2507, fewer mcirocracks are observed in SAF 2906 which are also located within a shallower surface layer (Fig. 3c). This could be explained by a higher stress level with respect to its yield strength (120% $R_{p0.2}$). Severe plastic deformation in the ferritic phase may lead to a faster failure process with less time for the development of hydrogen damage. Although voids are found at both phase and grain boundaries at large depth, they seem to promote crack initiation and propagation near the surface. Cleavage on the {100} plane as the main mechanism has also been identified as shown in Fig. 3c. The surface crack starting in grain 2 grows along a {100} plane. Phase boundaries with small angle to the loading direction also stop the HISC.

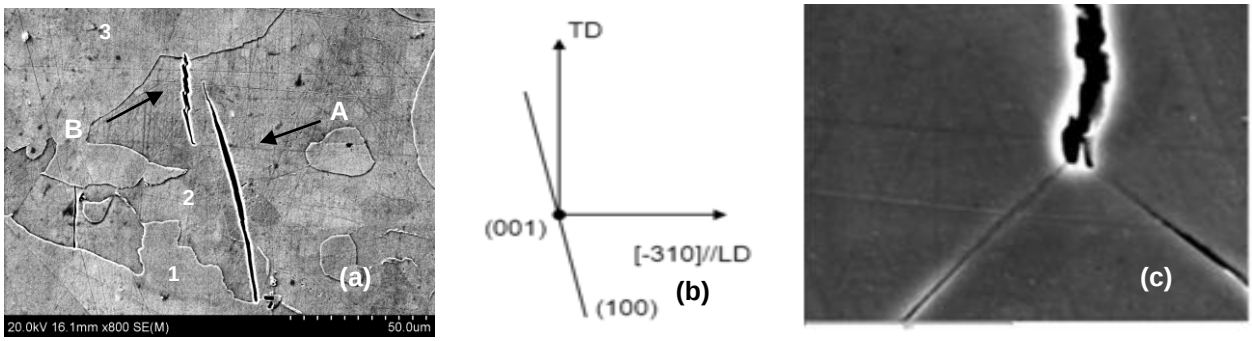

Fig. 4 (a). Cracks in grain 2, the small crack to the left is in a neighboring ferritic grain, (b). Sketched orientation of the grain, (c). Hydrogen concentration induced cleavage.

The main mechanism for crack propagation in ferrite is cleavage. In some case, a sudden grain orientation change up to 7 or 8 degrees across the crack is observed, which could mean that the crack propagates along low angle ferritic boundaries. Anyhow, for cleavage cracking, the propagation path can take different forms, as revealed in Fig. 4 a, and also sketched to the right of the figure (Fig. 4b). Crack A starts from the phase boundary and grows into the ferrite via cleavage of {100} planes, which leads to a smooth crack path. Crack B shows saw tooth geometry with the step planes parallel to the {100} plane trace. It is observed in other ferritic grains that the formation of a "tooth" is via the re-initiation of a new crack, ahead of the crack tip and on parallel planes, and is linking to the main crack. For grain 2, crack traces are found to agree also with the {100} planes. Fig. 4c shows a possible hydrogen concentration induced cleavage (HEDE) in the ferritic phase.

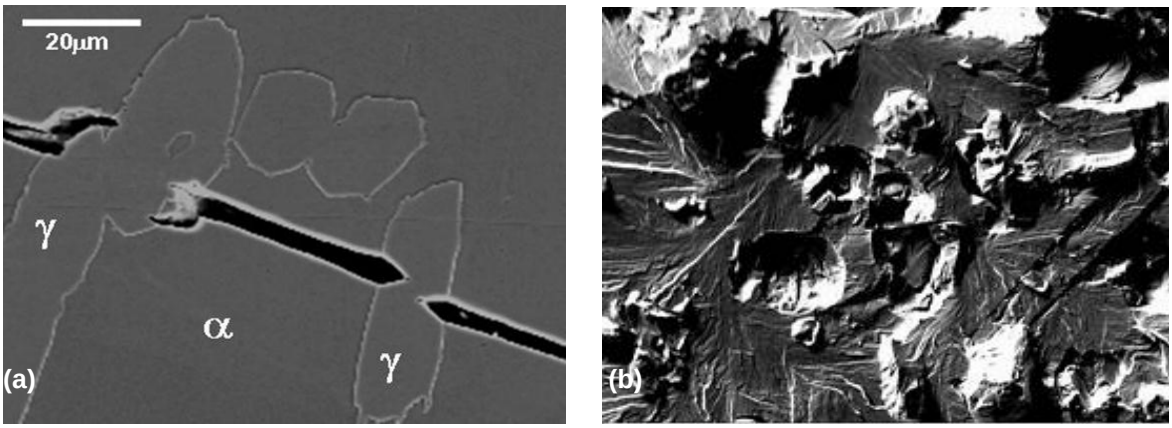

Fig. 5 Discontinuous cracking path in duplex stainless steels. (a). Crack path, SAF 2906, (b). "Valleys" and "peaks" fracture surface of SAF 2507.

The crack propagation during the HISC in DSS can be described as discontinuous crack growth, since the austenitic phase acts as an obstacle for crack propagation. As can be seen in Figure 5a, a crack can be "stopped" at one side of an austenitic grain, but will continue to propagate from the other side of the grain along the same direction. Crack deflection, branching and new crack initiation can also occur at phase boundaries. Consequently, the fracture surface covers "valleys" and "peaks" (Figure 5b). The cleavage fracture (smooth surface) is usually the ferritic phase, while the peak or valley is the austenitic phase with facet or quasi-cleavage fracture.

Heterogeneous deformation in duplex stainless steels. As shown in Fig. 1, micro deformation behaviors in duplex stainless steels are very different. These three materials show three phenomena. SAF 2205 can be treated as having more or less homogeneous deformation behaviors in the material although the two phases have totally different deformation mechanisms. Fig. 6 shows schematic deformation processes for other two DSS with inhomogeneous deformation behavior during the HISC test. For SAF 2507 as shown in Fig. 6a, at a given stress, σ, near the yield strength of the bulk DSS, the austenitic phase can yield at once with a tensile strain of ε_γ.The strain in the ferritic phase is ε_α. However, they have to approach to the bulk strain ε_b in order to keep the continuality of the system. Consequently, the austenitic phase will undergo a stress that is lower than the applied stress (σ) and the ferritic phase has a stress that is higher than the applied stress. This indicates that the austenitic phase will not deform further under the HISC test, but the ferritic phase will creep. Since the hardness or yield strength of both phases is similar, this can lead to the damage occurred mainly in the ferritic phase. Fig. 6b shows the situation for SAF 2906, which now is just the opposite. The ferritic phase is a softer phase and has a lower deformation hardening rate, and therefore will undergo a higher and severe plastic deformation ($\varepsilon_\alpha - \varepsilon_{\alpha 0}$) and suffer from HISC during the test. However, the austenitic phase will also creep, but comparatively small since it has a higher hardness or strength (Table 1).

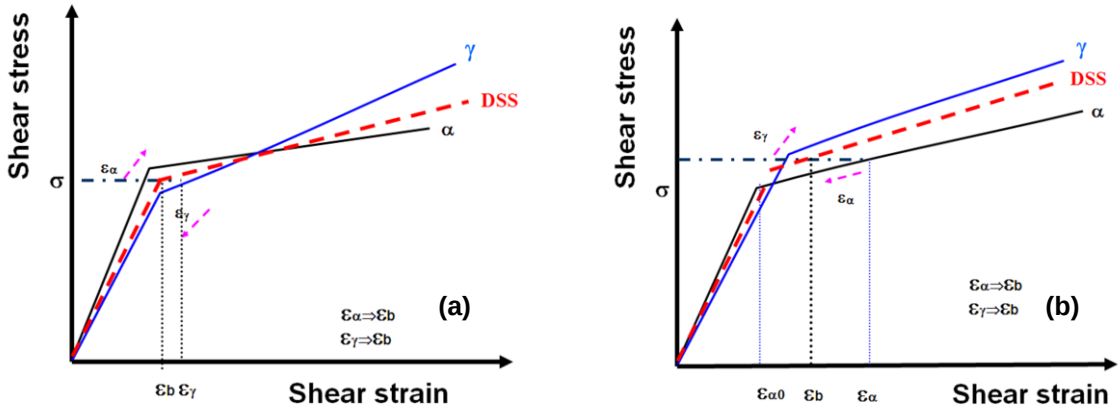

Fig. 6 A schematic deformation process during the HISC test with a constant stress, σ□ (a). In SAF 2507 (b). In SAF 2906.

Fig. 7 shows EBSD maps of these three materials after the HISC tests. SAF 2205 (Fig. 7a) has high dislocation densities, evident by the high density of low angle grain boundaries (LAGB), in both phase. As mentioned previously, SAF 2205 has a more homogeneous deformation in both phases, and therefore suffers from HISC damage in both phases (Fig. 2a and 3a). SAF 2507 has a higher dislocation density in the ferritic phase and at the phase boundaries (Fig. 7b) where the plastic deformation and also HISC damage is highest (Fig. 2b and 3b). While in SAF 2906, dislocations are more concentrated in the ferritic phase and at the phase boundaries, high dislocation density in the austenitic phase can also be observed, which is the result of the creep deformation during the HISC

test. Therefore, HISC damage occurs mainly in ferritic phase but can also occur in the austenitic phases (Fig. 3c and 3c).

The above observations and results indirectly verify the interactions between the hydrogen atoms and dislocations in these three materials. HISC is controlled by both plastic deformation introduced by loading and plastic deformation introduced by creep during the HISC testing. The above discussions show that the occurrence of HISC is a result of the interaction between the static and dynamic plasticity and hydrogen, whether the applied stress is lower or higher than the yield stress.

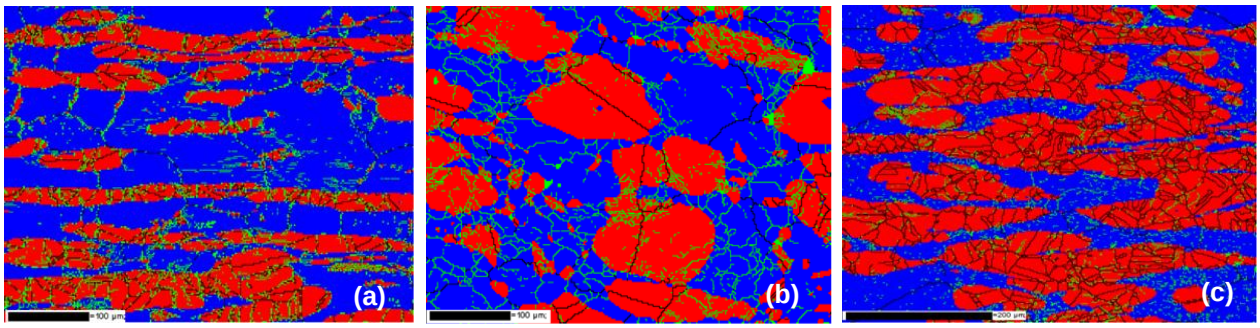

Fig. 7 Phase structure with austenite (red) and ferrite (blue) after the HISC testing. The green lines are low angle grain boundaries (between 2 and 10 degree); (a). SAF 2205, (b) SAF 2507, (c). SAF 2906.

Conclusions

Deformation in duplex stainless steels is very heterogeneous in micro scale depending on material chemical compositions.

HISC in duplex stainless steels depends strongly on the material composition, microstructure and loading conditions. HISC is a result of the interaction between the static and dynamic plasticity and hydrogen.

HISC damage (voids) can occur in both austenitic and ferritic phases and at both grain boundaries and phase boundary depending on plastic deformation introduced by both loading and creep and hydrogen diffusion during the HISC test.

The crack propagation paths in the DSS during HISC are discontinuous. The fracture surface consists of the cleavage valleys of the ferritic phase and the peaks of the austenitic phase. This is mainly due to the heterogeneous mechanical behavior of these two phases.

Acknowledgements

This paper is published by permission of Sandvik Materials Technology. The authors are also indebted to the co-authors in the reference list for their contribution and collaborations.

References

[1] NORSOK Workshop Agreement M-WA-01 Rev. 1, “Design guideline to avoid hydrogen induced stress cracking in subsea duplex stainless steels” (Lysaker, Norway: Standard Norway, 2005)

[2] Design guideline for duplex stainless steel used for subsea equipment exposed to cathodic protection.” Report No.2005-3237, (Hövik, Norway: DNV, 2005)

[3] R. Oltra, C. Bouillot, and T. Magnin: Scirpta Materialia 35 No. 9 (1996), p.1101.

[4] P. Woolin and W. Murphy: Stainless Steel World, (June 2001), p. 48.

[5] M. Yoshoka, A.Ueno and H. Kishimoto: J. Soc. Mat. Sci., Japan, 52 (2003), p. 660.
[6] S. Ronneteg, A. Juhlin and U. Kivisäkk: (2006), EUROCORR 2006.
[7] G. Chai, S. Ronneteg, U. Kivisäkk, R. Lin Peng and S. Johansson: Steel research int. 80 No. 7 (2009), p. 485.
[8] S. P. Lynch: (2007), NACE, No. 07493.
[9] O. Haukas-Eide, B. Hugaas, and E. Heier, (2007), NACE, No. 07494.
[10] R. Lillbacka, G. Chai, M. Ekh, P. Liu, E. Johnsson and K. Runesson, Acta Materialia, 55 (2007), P. 5359
[11] N. Jia, R. Lin Peng, Y. D. Wang, G. C. Chai, S. Johansson, G. Wang and P. K. Liaw: ACTA Materialia, 54 (2006) p. 3907
[12] N. Jia, R. Lin Peng, G. Chai, S. Johansson and Y. D. Wang: Materials Science and Engineering A 491 (2008) p. 425.